Vol. 23, No. 1(2024) Alim24109
Revista Mexicana de Ingeniería Química

Development of modified cassava starches by ultrasound-assisted amylose/lauric acid complex formation

Desarrollo de almidones modificados de yuca mediante la formación de complejos amilosa/ácido láurico asistido por ultrasonido

V Ramos-Villacob*, J.A. Figueroa-Flórez, J.G. Salcedo-Mendoza, J.E. Hernandez-Ruydíaz, L.A. Romero-Verbel
Department of Engineering, University of Sucre. Cra. 28 #5-267, Sincelejo-Sucre
Received: July 19, 2023; Accepted: November 9, 2023

Abstract
Tuber starches have a smooth surface and a dense amylopectin structure, which prevents the formation of complexes with lipid compounds. The present study evaluated the effect of ultrasound on the formation of starch-lipid complexes on cassava starch's structural, morphological, physicochemical, and digestibility properties. Lauric acid was added at concentrations of 0.075 and 0.15 % w/v to previously swollen cassava starch suspension (60 °C, 1 h), and the mixtures were stirred and heated in an ultrasonic bath at 60 °C (power 100W, frequency 37 and 80 kHz for 1 h). The starch modification was confirmed by infrared spectroscopy, showing the presence of the C=O group. The modified starches presented a V-type crystalline structure and lower crystallinity due to the modification conditions, lauric acid concentration, and ultrasonic effect. Deformations and partial ruptures of starch granules were observed under microscopy. In addition, the modified starches showed decreased amylose content and solubility in cold water, higher stability during heating, and lower retrogradation, attributed to the presence of lipids. There was also an increase in resistant starch content due to the formation of complexes. In conclusion, ultrasound is a promising technique for driving the formation of cassava starch-lauric acid complexes, with modified properties which may be expand their potential use in the food industry.
Keywords: Starch-lipid complex, cassava, sonication, frequency, digestion.

Resumen
Los almidones de tubérculos tienen una superficie lisa y una estructura densa de amilopectina, lo que evita la formación de complejos con compuestos lipídicos. El presente estudio evaluó el efecto del ultrasonido en la formación de complejos almidón-lípido sobre las propiedades estructurales, morfológicas, fisicoquímicas y de digestibilidad del almidón de yuca. Se agregó ácido láurico en concentraciones de 0.075 and 0.15 % w/v a una suspensión de almidón de yuca previamente hinchada (60 °C, 1 h), y las mezclas fueron agitadas en un baño ultrasónico a 60 °C (potencia 100 W, frecuencia 37 y 80 kHz, 1 h). La modificación del almidón se confirmó por espectroscopía infrarroja, mostrando la presencia del grupo C=O. Los almidones modificados presentaron una estructura cristalina tipo-V y menor cristalinidad debido a las condiciones de modificación, concentración de ácido láurico y efecto ultrasónico. Se observaron deformaciones y rupturas parciales de los gránulos de almidón bajo microscopía. Además, los almidones modificados mostraron disminución en contenido de amilosa y solubilidad en agua fría, mayor estabilidad durante el calentamiento y menor retrogradación, atribuidas a la presencia de lípidos. También se registró aumento en contenido de almidón resistente debido a la formación de complejos. En conclusión, el ultrasonido es una alternativa prometedora para la formación de complejos con ácido láurico, ofreciendo un producto con nuevas propiedades con potencial de aplicación en la industria de alimentos.
Palabras clave: Complejo almidón-lípido, yuca, sonicación, frecuencia, digestión.

*Corresponding author. *E-mail*: veronica.ramos@unisucre.edu.co;
https://doi.org/10.24275/rmiq/Alim24109
ISSN:1665-2738, *issn-e*: 2395-8472

1 Introduction

Cassava crops play a crucial role in Colombia, both socially and economically, and in terms of food security, especially in regions with high production. They serve as the primary source of income and food for the population. However, cassava is predominantly consumed in fresh, and there is an ongoing drive seeking to develop alternative products from cassava and diversify its potential industrial usage. Cassava tubers possess high starch content with versatile physicochemical properties, making them a valuable functional ingredient (Zhong *et al*., 2020). Natural cassava starch is important due to its wide range of applications, low cost, availability, renewability, biodegradability, and gel-forming ability (Arenas & Pedraza, 2017). However, in its natural form, it exhibits low solubility in cold water, high retrogradation, liquid separation from pastes, limited emulsifying capacity, and resistance to chemical and enzymatic modifications, among others (Zhang *et al*., 2021).

Starch modification has emerged as a revolutionary processing technology, which can improve the functional properties of starchy materials. Modification methods include chemical, physical, enzymatic, and genetic processes (Cao *et al*., 2023). The production of starch-lipid complexes stands out as a harmless modification approach, relying on the interaction between natural polymers to form a composite system with unique processing characteristics and distinctive functional properties (Oyeyinka *et al*., 2021). The formation of starch-lipid/fatty acid complexes leads to changes in the morphological structure, physicochemical and rheological properties, and on the digestibility of starch, thereby influencing its industrial application by introducing novel functionalities such as reduced digestibility, its use a bioactive carrier with controlled release capability, and as fat substitute, among others (Jin, 2018).

The use of high-speed homogenization has been reported as being an efficient method for driving the formation of complexes between linear starch chains and lipid compounds. On the other hand, ultrasonication has emerged as a promising non-thermal technology, which improves lipid dispersibility in starch (Kang *et al*., 2020). The ultrasonic waves induce the release straight-chain amylose molecules and ultrasound is considered a "green technology". Starch modification is achieved when using high-frequency waves exceeding 16 kHz (Wang *et al*., 2020). Several researchers have documented that ultrasound has the potential to modify the physicochemical characteristics of starch, including changes such as depolymerization or polymerization, alterations in water vapor permeability, variations in gelatinization temperature, modifications in swelling power, adjustments in viscosity and changes in solubility (Xiao *et al*., 2021).

Despite that ultrasonication has been widely employed for inducing starch modification, the mechanisms by which ultrasound affects starch-lipid complexes' physicochemical, structural, and digestibility properties remains not fully understood.

The aim of this study was to systematically investigate the formation mechanism of starch-lipid complexes through ultrasonication at different frequencies and lipid concentrations, and to examine the impact of ultrasound on the physicochemical, morphological, structural, and digestibility properties of cassava starch-lauric acid inclusion complexes.

2 Materials and methods

2.1 Materials

Native cassava starch (*Manihot esculenta* Cv M-TAI) was provided by Almidones de Sucre S.A.S (Sincelejo-Colombia). Lauric acid (purity ≥ 98 %, in solid state at room temperature) was supplied by Sigma-Aldrich® St. Louis, MO., USA. Enzymatic polypeptides of bacterial α-amylase (Lyquozyme Supra-2.2X®) and fungal amyloglucosidase (Dextrozyme® GA) were provided by Novozymes® (Bagsvaerd, Denmark). Porcine pancreatic α-amylase, with biocatalytic activity ≥ 5 U/mg (Sigma-Aldrich®, Type VI-B, USA) was used.

2.2 Ultrasound-assisted preparation of starch-lipid complexes

Starch-lauric acid complexes were formed following the methodology proposed by Raza *et al*. (2021) with some modifications. A starch suspension (5.5 % w/v, dry starch base, dbs) was prepared in a water bath below the gelatinization temperature of cassava starch. The starch pasting temperature was recorded at 69.63 °C according to the rheometer pasting curves (MCR 302, Anton Paar, Austria) Chang *et al*. (2013). Therefore, the suspension was heated to 60 °C with vigorous stirring for 1 h. Subsequently, lauric acid dissolved in ethanol was added to the swollen starch dispersions with lauric acid concentrations of 0.075 and 0.15 % w/v. Then, the mixtures were stirred and heated in an ultrasonic bath at 60 °C, with a power of 100 W and ultrasonic frequency of 37 and 80 kHz for 1 h. Afterward, the mixtures were cooled to room temperature for 30 min, and excess water was removed by separation through centrifuging and washing twice with 70% ethanol and two washes with distilled water for 5 min. Finally, the precipitates were dried in an

oven at 35 °C for 18 h, macerated, passed through a 200 mesh, stored, and labeled. Samples without ultrasound treatment at different concentrations of 0.075 and 0.15 % were labelled SLC-C1 and SLC-C2 respectively, referring to the starch-lipid complexes formed at concentrations 1 and 2. While the samples treated with ultrasound were named CUC1 and CUC2, referring to the complex treated with ultrasound at concentrations 1 and 2 (0.075 and 0.15 %) followed by the value of the frequency used (CUC1-37, CUC1-80, CUC1-37 and CUC1-80) and the control treatment that makes the native cassava starch was named NCS.

2.3 Complex index

The complex formation index (CI) value was determined using the method of de Kang *et al*., (2020). Initially, a 10% w/v starch suspension was heated at 95 °C for 30 min. Subsequently, 5 g of the starch paste was diluted in 25 mL of distilled water and vibrated in the vortex for 120 s. The sample was then centrifuged at 4500 rpm for 15 min and diluted with distilled water (D:4). Afterward, 500 μL of the dilution was collected in a test tube previously lined with sugar paper, 15 mL of distilled water was added and mixed with 2 mL of iodine solution. The absorbance values of the samples were determined with a UV-VIS Pharo 300 spectrophotometer (Spectroquant®, Darmstadt, Germany) at 690 nm. The CI values were expressed as a percentage and estimated by the following equation:

$$CI(\%) = \frac{ABS_{reference} - ABS_{sample}}{ABS_{reference}} * 100\% \qquad (1)$$

Where $ABS_{reference}$ and ABS_{sample} are the absorbance values of native starch and starch-lipid complex, respectively.

2.4 Apparent amylose content

Amylose content was determined by iodine adsorption spectrophotometry (Serna-Fadul, 2022) with the following modification: Starch samples were dissolved/degreased in 95% DMSO solution and subsequently precipitated in 90% methanol. The sample was reacted with an I2/KI solution for 10 min. Then, from a calibration curve of standard solutions of potato amylose and corn amylopectin under concentrations of 0-100% w/w, the absorbance value of the amylose/iodine colorimetric reaction was determined at 620 nm.

2.5 Attenuated total reflectance Fourier transform infrared

Infrared spectra of the samples were acquired using a Fourier Transform Spectrometer equipped with an ATR accessory (UATR, Pelkin Elmer, USA) with a 1.5 mm diameter diamond crystal. FTIR-ATR spectra were obtained within a wavenumber range of 400 to 4000 cm^{-1} and a resolution of 8 cm^{-1}.The data were processed by Spectrum software (Perkin Elmer, version 10.7.2, USA). The absorbance ratios 1047/1022 cm^{-1} and 995/1022 cm^{-1} were determined to estimate the variations in the molecular order of each sample (Reyes *et al*., 2023).

2.6 X-ray diffraction

X-ray diffraction patterns of the samples were obtained using a diffractometer (X'Pert Pro- MPD, Panalytical, Italy). The parameters used for the test were: 1.8 kW, 40 mA, and CuK beams (λ = 1.55 pm) with scanning in the Bragg 2θ angle range of 5-40° and a scanning speed of 2 °/min and sampling interval of 0.02°. The degree of crystallinity was calculated from the ratio of crystalline area to total diffractogram area obtained by numerical integration methods in MATLAB R2019a software (MathWorks, R2019a, USA) (Zhou *et al*., 2023).

2.7 Pasting properties

To determine the viscosity profile of the starch pastes, a viscoamylogram was performed, applying the technique used by Chandak *et al*., (2022) with slight modifications. A rotational mode rheometer (MCR 302, Anton Paar, Austria) was used and 8 % w/v starch suspensions were subjected to different temperatures. The heating and cooling conditions were 50 °C for one min, heating to 95 °C in 7.5 min, holding at 95 °C for 5.0 min, cooling to 50 °C in 7.5 min, and finally a holding at 50 °C for two minutes. The spindle speed was (ST24-2D/2V/2V-30, Anton Paar, Austria) 250 rpm. The parameters evaluated were: pasting temperature (PT), peak viscosity (PV), final viscosity (FV), breakdown (BD), and setback (SB).

2.8 Scanning electron microscopy

The granular morphology of the starches was analyzed in a scanning electron microscope (JEOL, JSU-5600 LV, Japan). Starch samples were coated in with gold with a thin film sputtering unit (model Desk V, Denton Vacuum) (Salgado-Delgado *et al*., 2022). Samples were observed under a scanning electron beam column, operating at 10 eV voltage acceleration in an ultra-high-vacuum. Selected micrographs at different magnifications are presented.

2.9 Thermal analysis

The gelatinization properties of the samples were evaluated using a differential scanning calorimeter (DSC-Q200, TA Instruments, USA) and following the methodology of Alpizar-Reyes *et al*., (2022) with

slight modifications. Initially, a starch suspension was prepared in pre-weighed aluminum capsules under a 1:3 starch/water ratio (3 mg starch, d.b., and 9 mg distilled water). The aluminum capsules were then sealed and kept at room temperature for 24 h to homogenize the system. Afterward, the samples were subjected to heating from 20 to 120 °C at a rate of 10 °C/min and cooled at a ramp of 20 °C/min. The gelatinization temperatures were obtained from the thermograms and expressed in ºC. The enthalpy of gelatinization (ΔH) was estimated using TA Software (TA Instruments, USA) and expressed in J/g.

2.10 Solubility in cold water and swelling power

Cold water solubility (CWS) and swelling power (SP) values of native and modified starch followed the methodologies of Dewi *et al*. (2022) and Ge *et al*. (2022), respectively, with some modifications. To determine PBS, a starch suspension was stirred in 1.0 % w/v water for 5 min and at room temperature of 25 °C. It was then centrifuged at 4500 rpm for 15 min. The supernatant was poured into a previously weighed Petri dish and dried at 110 °C for 4 h. The supernatant weight was estimated to constant weight and the solubility in cold water was expressed as a percentage based on mass gain. While the swelling power was estimated by heating a 4 % w/v starch suspension with preheated distilled water at 60 °C, placed in a water bath at 60 °C for 30 min, centrifuging the sample, and determining the weight of the gel and the amount (g) of dry solids recovered by evaporation of the supernatant.

2.11 In vitro starch digestibility

The fractions of the rapidly-digested starch (RDS) content, slowly-digested starch (SDS) content, and resistant starch (RS) content were estimated following the methodology employed by Figueroa-Flórez, (2020). Initially, starch suspensions of 0.8 % w/v at 0.1 M citrate buffer solution (pH= 5.2) were heated for 20 min at 90 °C. The samples were then hydrolyzed with 1 mL of enzymatic solution consisting of 54 mL of pancreatic α-amylase (0.15 % w/v) and 6 mL of fungal amyloglucosidase (140 AGU/mL) at a temperature of 37 °C for 120 min and inactivated using 2 mL of 70 % ethyl alcohol. Aliquots were taken at 20 and 120 min to determine the released glucose content, using the DNS (dinitrosalicylic acid) method. The percentages of RDS, SDS, and RS were determined by the following equation:

$$RDS\,(\%) = \left[\frac{G_{20} - G_L}{G_T}\right](0.9)(100) \tag{2}$$

$$SDS\,(\%) = \left[\frac{G_{120} - G_{20}}{G_T}\right](0.9)(100) \tag{3}$$

$$RS\,(\%) = \left[\frac{G_T - G_L}{G_T}\right](0.9)(100) - (RDS) - (SDS) \tag{4}$$

Where G_{20} and G_{120} indicate the glucose content released after 20 and 120 min of hydrolysis, respectively. G_L represents the free glucose content and G_T is the total glucose content and 0.9 a glucose-to-starch conversion factor.

2.12 Statistical analysis

A factorial design was established where the factors evaluated were ultrasonic frequency and fatty acid concentration. All experiments were carried out in triplicate and the results were expressed as the mean ± standard deviation of the replicates. Differences between treatment means were evaluated using the statistical tool analysis of variance ANOVA and Tukey's statistical test with a significance level of 0.05. Statistical analysis was performed using Statgraphics Centurion software (Statgraphics Inc., version XVI, USA).

3 Results and discussion

3.1 Complexing index of starch-lipid complexes

The complex formation index (CI) represents the degree of lipid inclusion in the amylose helical cavity and is estimated based on the iodine binding capacity in the reduced cavity of the complex (Table 1). The results revealed a statistically significant increase in the rate of complex formation at high lauric acid concentrations in the non-ultrasound treatments, with SLC-C2 outperforming SLC-C1 with a CI value of 31.02%; possibly because a high proportion of dispersed lipids in the solution have a greater capacity to interact with free amylose. This result agrees with the data reported by Li *et al*. (2019), where they found that as the amount of palmitic acid increased the CI values increased until reaching saturation with a value of 28%.

On the other hand, the CI values increased with the implementation of the ultrasonic system for both lauric acid concentrations. These results could be because the ultrasonic vibration affected the semicrystalline order of the starches and this induced an improvement in the ability of complex formation between the compounds. This result was similar to that reported by Kang *et al*. (2020) where the cavitation effect of ultrasound promoted further dissolution of swollen starch granules, causing more amylose molecules to be released from the internal structure of starch and facilitating their interaction with the lipid molecule. In

turn, the ultrasonic effect improved the modification process by increasing the CI values by 22.38 and 13.12 %. Chumsri *et al*. (2022) stated that, when an ultrasound system is implemented, the linear amylose chains are detached from the amylose/amylopectin complexes, reorganizing the internal structure and increasing their participation in the formation of starch-lipid complexes.

Similarly, it was identified that starches treated with ultrasound showed significant differences in the CI at the two frequencies evaluated, resulting in a higher CI for starches treated at the frequency of 37 kHz than at 80 kHz. This result may be associated with the fact that treatments at high frequencies are usually softer and quieter than ultrasonic treatments at low frequencies, hence, damage to starch macromolecules is milder, thus preventing further release of amylose to interact with lauric acid. Raza *et al*. (2021) also found that when ultrasonic treatment increased to frequencies higher than 40 kHz the rates of complex formation between *Sagittaria sagittifolia* starch and linoleic acid decreased from 83.9 to 76.7 %. These results could explain the physicochemical, pasting, and *in vitro* digestibility properties of the complexes.

3.2 Apparent amylose content (AC)

The results of the apparent amylose content of native starch and starch-lipid complexes are depicted in Table 1. The native cassava starch presented an amylose content of 24.21%, this value agrees with the results reported by Rolland-Sabaté *et al*. (2012) who reported a range of amylose content varying from 16.8 to 30.3 % in cassava starches for the variety "M-TAI18", these values depend on the origin, variety, harvesting time and type of isolation of the starchy material (Méndez *et al*., 2022). Apparent amylose content showed a statistically significant decrease ($p<0.05$) after starch modification, which could indicate that the formation of the starch complex with lauric acid reduced the availability in the amylose helical cavity, preventing amylose from forming complexes with iodine and confirming that there was entrapment of lauric acid in the amylose structure (Tufvesson *et al*., 2003). In addition, it was observed that as the lauric acid concentration increased, the amount of amylose present in the starch was reduced, showing an inverse relationship with the values reported by the complex formation index. Similar results were found by Faridah *et al*. (2021) who indicated that complexes formed at higher lauric acid concentrations could form complexes with starch more easily.

On the other hand, the results revealed that when the ultrasound system was implemented, the amylose content in the complexes was higher concerning the modification without ultrasonic induction, which may be related to the fact that the ultrasonic effect causes a molecular reorganization, increasing the availability of the number of amylose molecules for the formation of complexes with lauric acid. Golkar *et al*. (2023) explained that corn starch after being modified by ultrasound increased the amylose content due to the fractionation of amylose and amylopectin molecules that reduced the length of both molecules accelerating the reaction between starch and iodine. In turn, Xiao *et al*. (2021) point out that modification with ultrasound increased the apparent amylose content in native potato starches because the ultrasonic frequency disrupted the α-1,6 glycosidic bonds of the amylopectin branch point, and also broke into long branching chains, leading to the appearance of more linear amylose chains. Consequently, this could explain the behavior of increased amylose content during complex formation with ultrasonic systems.

Table 1. Physicochemical properties of starch-lauric acid complexes.

SAMPLE	CI	AC	CWS	SP
NCS	——	24.21 ± 0.81^{a}	1.81 ± 0.18^{a}	2.08 ± 0.01^{a}
SLC-C1	28.47 ± 0.27^{a}	21.99 ± 0.39^{b}	1.49 ± 0.05^{b}	2.19 ± 0.01^{b}
CUC1-37	50.85 ± 0.18^{b}	23.66 ± 0.30^{a}	0.37 ± 0.05^{c}	2.52 ± 0.00^{c}
CUC1-80	46.95 ± 0.33^{c}	26.75 ± 0.26^{c}	1.15 ± 0.05^{de}	2.43 ± 0.02^{d}
SLC-C2	31.02 ± 0.50^{d}	15.91 ± 0.76^{d}	1.73 ± 0.05^{a}	2.74 ± 0.03^{e}
CUC2-37	44.14 ± 0.63^{e}	18.30 ± 0.07^{e}	0.99 ± 0.05^{e}	2.26 ± 0.02^{f}
CUC2-80	35.76 ± 0.33^{f}	17.07 ± 0.29^{de}	1.31 ± 0.05^{bd}	2.55 ± 0.03^{c}

CI: complex formation index; AC: apparent amylose content; CWS: cold water solubility; SP: swelling power; NCS, native cassava starch; SLC-C1, starch-lipid complex with 0.075% lauric acid without ultrasound; SLC-C2, starch-lipid complex with 0.15% lauric acid without ultrasound; CUC1-37, starch-lipid complex with 0.075% lauric acid and ultrasound at 37 kHz; CUC2-37, starch-lipid complex with 0.15% lauric acid and ultrasound at 37 kHz; CUC1-80, starch-lipid complex with 0.075% lauric acid and ultrasound at 80 kHz; CUC2-80, starch-lipid complex with 0.15% lauric acid and ultrasound at 80 kHz.

3.3 FTIR-ATR spectroscopy

FTIR-ATR spectra revealed changes in the characteristic absorption bands of starchy materials after the formation of starch-lipid complexes, suggesting possible changes in the molecular order of starch granules (Fig. 1). The bands in the 800-1500 cm^{-1} and 1500-4000 cm^{-1} range in the FTIR-ATR spectrum represent the fingerprint region and the diagnostic zone, respectively (Figueroa-Flórez, 2020). All fatty acid-modified starch samples exhibited bands around 2850 cm^{-1} and 2927 cm^{-1}, which correspond to the asymmetric stretching vibration of the -CH_2 and -CH_3 groups in the fatty acid alkyl chain (Chumsri *et al*., 2022). In turn, the samples presented a broad band in the range of 3000-3700 cm^{-1}, which was attributed to the O-H stretching vibration associated with the hydroxyl groups of starch (Li *et al*., 2021). The treatments by starch-lipid complex formation and sonication caused varying degrees of shift of the peak at 3428 cm^{-1}, corresponding to C-H absorption, caused by CH, CH_2, and CH_3 stretching and bending vibrations (Tang *et al*., 2022). These results were similar to those found for yam starch and palmitic acid complexes (Li *et al*., 2019).

The characteristic peak of lauric acid was observed around the approximate 1690 cm^{-1} bands corresponding to the C=O carbonyl group. When lauric acid formed complexes with amylose, the characteristic C=O peak shifted to approximately 1650 cm^{-1}. Similar results were reported by Chumsri *et al*. (2022), who point out that this band could result from breaking hydrogen bonds between the carboxyl groups of fatty acids in the crystalline state, suggesting that fatty acids are incorporated into the amylose helix. Similarly, the results showed a decrease in the band intensities of modified starches concerning their native counterpart. This decrease was more evident for starches treated with ultrasound and higher concentrations of lauric acid. Raza *et al*. (2022) claim that the decrease in intensity of the bands could be due to the increased hydrophobicity of the starches as a result of the action of lipids and ultrasound, which is consistent with the IC results determined by XRD.

In the fingerprint region, the crystalline region is highlighted by absorption peaks at 1047 cm^{-1} and 995 cm^{-1}, while the amorphous region is represented by the absorption peak at 1022 cm^{-1}. The short-range order of helical structures and potential internal changes in the double helices of starch granules can be revealed through changes in the absorbance ratios of 1045/1022 cm^{-1} (OM1) and 995/1022 cm^{-1} (OM2), respectively. Starches modified with lauric acid showed decreased values of OM1 and OM2 compared to their native counterpart (Table 2), indicating that the starch-lauric acid complexes possessed a lower degree of short-range molecular order compared to native cassava starch, which aligns

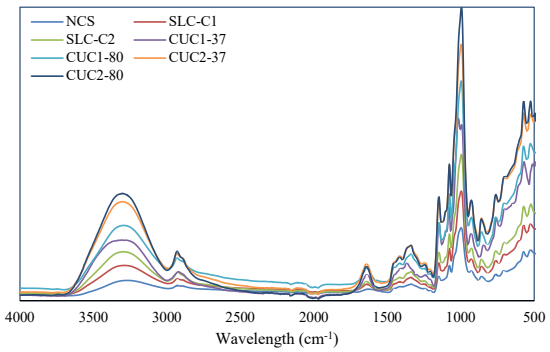

Figure 1. Fourier transformation infrared spectroscopy of native and modified cassava starch. NCS, native cassava starch; SLC-C1, starch-lipid complex with 0.075% lauric acid without ultrasound; SLC-C2, starch-lipid complex with 0.15% lauric acid without ultrasound; CUC1-37, starch-lipid complex with 0.075% lauric acid and ultrasound at 37 kHz; CUC2-37, starch-lipid complex with 0.15% lauric acid and ultrasound at 37 kHz; CUC1-80, starch-lipid complex with 0.075% lauric acid and ultrasound at 80 kHz; CUC2-80, starch-lipid complex with 0.15% lauric acid and ultrasound at 80 kHz.

with the data reported by XRD. This reduction may be attributed to the interaction and association between lauric acid molecules and starch molecules, disrupting the starch's crystalline structure and causing its disorganization (Wang *et al*., 2018). Additionally, the decrease in OM could suggest that the modified starches likely had a V-type single-helix pattern of amylose (D'Silva *et al*., 2011). These results differ from those reported by Chumsri *et al*. (2022), Li *et al*. (2019), Raza *et al*. (2022), and Tang *et al*. (2022) who found that at the absorbance ratio 1045/1022 cm^{-1} of native starches increased upon forming complexes with fatty acids. The difference between our results and those of the aforementioned authors may be due that the latter used higher temperatures (higher than those required for complete gelatinization) than the former, so that a higher amylose release took place, resulting in a more ordered granule structure.

3.4 X-ray diffraction (XRD)

The X-ray diffraction patterns of native and modified cassava starches can be observed in Fig. 2. The native cassava starch samples presented a diffraction pattern characteristic of a type-A polymorphism, exhibiting crystalline peaks at Bragg angles: 11, 15, 17, 17, 18 and 23°, behavior similar to those reported by Faridah *et al*., (2021). After modification of native starch with lauric acid a new peak of intensity 2θ = 20 was identified which was attributed to a well-formed V-type structure, which was assigned to closely packed individual amylose helices complexed with various polar and non-polar compounds, such as fatty acids

Table 2. Molecular order and *in vitro* digestibility for native and modified starches.

SAMPLE	OM1	OM2	RDS(%)	SDS(%)	RS (%)
NCS	0.7240 ± 0.0039^{b}	1.3105 ± 0.0179^{a}	72.98 ± 1.13^{a}	17.06 ± 0.62^{a}	9.96 ± 0.50^{a}
SLC-C1	0.7137 ± 0.0014^{c}	1.2364 ± 0.0003^{c}	44.98 ± 0.73^{b}	43.33 ± 0.07^{b}	11.69 ± 0.73^{b}
CUC1-37	0.6537 ± 0.0036^{e}	1.1198 ± 0.0089^{e}	36.48 ± 0.11^{c}	44.61 ± 0.08^{c}	18.90 ± 0.19^{c}
CUC1-80	0.7173 ± 0.0005^{bc}	1.2283 ± 0.0048^{c}	75.61 ± 0.60^{d}	10.87 ± 0.01^{d}	13.52 ± 0.61^{d}
SLC-C2	0.6971 ± 0.0043^{d}	1.2714 ± 0.0003^{b}	69.64 ± 0.38^{e}	14.16 ± 0.03^{e}	16.20 ± 0.41^{e}
CUC2-37	0.7325 ± 0.0035^{a}	1.2012 ± 0.0070^{d}	63.40 ± 0.32^{f}	20.42 ± 0.07^{f}	16.19 ± 0.39^{e}
CUC2-80	0.6949 ± 0.0016^{d}	1.2838 ± 0.0065^{b}	71.77 ± 0.17^{a}	17.22 ± 0.08^{a}	11.00 ± 0.09^{ba}

OM1, Ratio 1045/1022 cm^{-1}; OM2, Ratio 925/1022 cm^{-1}; RDS, rapidly digested starch; SDS, slowly digested starch; RS, resistant starch. NCS, native cassava starch; SLC-C1, starch-lipid complex with 0.075% lauric acid without ultrasound; SLC-C2, starch-lipid complex with 0.15% lauric acid without ultrasound; CUC1-37, starch-lipid complex with 0.075% lauric acid and ultrasound at 37 kHz; CUC2-37, starch-lipid complex with 0.15% lauric acid and ultrasound at 37 kHz; CUC1-80, starch-lipid complex with 0.075% lauric acid and ultrasound at 80 kHz; CUC2-80, starch-lipid complex with 0.15% lauric acid and ultrasound at 80 kHz.

(Chumsri *et al*., 2022). The formation of this new peak was much more intense in complexes with high concentrations of lauric acid, which may be attributed to a higher amount of complexed or free fatty acids in the starch matrix (Di Marco *et al*., 2023).

In addition, the non-ultrasonically treated samples exhibited weaker diffraction intensity than the ultrasonically treated starch-lipid samples, which indicated that the amount of the inclusion complex showed an increasing trend after exposure to ultrasonic treatment at frequencies of 37 and 80 kHz. Similar results were reported by Raza *et al*. (2021) and by Chumsri *et al*. (2022) who indicated that the use of ultrasound can drive structural changes including a rearrangement of linear amylose-amylose or amylose-amylopectin chains, affecting the semicrystalline order and enhancing the formation of V-type starches in *Sagittaria sagittifolia* and rice starches, respectively. Marinopoulou *et al*. (2016) indicated that amylose-fatty acid complexes prepared at temperatures near 60 °C were in an amorphous (type-I) state, whereas, at temperatures above 90 °C, the complexes were in a semi-crystalline (type-II) state. Therefore, it could be said that the modified starches presented a Type-I crystallization, a behavior similar to the studies reported by Zabar *et al*. (2010) and Chang *et al*. (2013) who formed complexes below the gelatinization temperature of starch in its native state.

Additionally, a decrease in the relative crystallinity of lauric acid-modified starches was observed compared to their native counterpart, with a decrease from 46.69 to 35.96% in the case of SLC-C2 complexes, as shown in Fig 2. These changes could be attributed to the partial swelling of the starch granules during the preheating process in water, which may have resulted in a widening of the pores of the native granule. This in turn allowed lauric acid to interact with amylose and interfere with the association of starch polymers, forming a less organized structure due to the steric hindrance of alkyl chains, which affected the recrystallization of starch molecules (Wang *et al*., 2018). This reduction was more noticeable in complexes formed with higher concentrations of lauric acid. However, an increase in relative crystallinity was observed in the ultrasound-treated complexes (CUC1-37, CUC1-80 and CUC2-80) compared to the untreated samples (SLC-C1 and SLC-C2). In this sense, the application of ultrasound at both frequencies in the process could have caused a cavitation effect resulting in partial depolymerization of amylose, breaking the α-1,6-glycosidic bonds of amylopectin and degrading the latter, in turn, could have led to an increase in the leaching of linear amylose chains that improved the structural order and led to stronger interactions between starch and lauric acid (Di Marco *et al*., 2023).

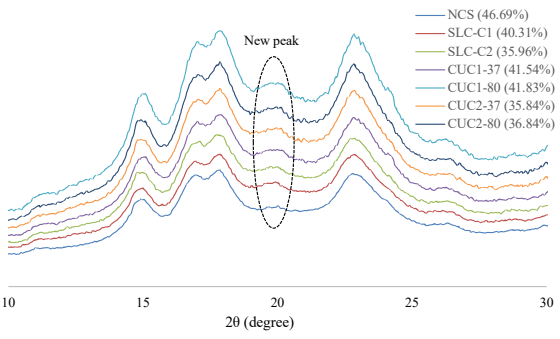

Figure 2. X-ray diffraction patterns of native and modified cassava starch. NCS, native cassava starch; SLC-C1, starch-lipid complex with 0.075% lauric acid without ultrasound; SLC-C2, starch-lipid complex with 0.15% lauric acid without ultrasound; CUC1-37, starch-lipid complex with 0.075% lauric acid and ultrasound at 37 kHz; CUC2-37, starch-lipid complex with 0.15% lauric acid and ultrasound at 37 kHz; CUC1-80, starch-lipid complex with 0.075% lauric acid and ultrasound at 80 kHz; CUC2-80, starch-lipid complex with 0.15% lauric acid and ultrasound at 80 kHz.

These results are consistent with morphological analyses performed on starch-lauric acid complexes. Previous studies have reported that fatty acid-modified starches below gelatinization exhibit a decrease in relative crystallinity in potato starches (Wang *et al*., 2018). However, Raza *et al*. (2021) reported that the use of ultrasound in complex formation increased the crystallinity of native starches from *Sagittaria sagittifolia*. These results are consistent with those obtained in the present investigation.

3.5 Scanning electron microscopy (SEM)

The morphology of the native cassava starch granules (NCS) exhibited mainly a spherical or oval shape, with a smooth surface showing no evidence of lacerations or porosities (Fig. 3). However, some of these starch granules may present minor surface damage, such as truncated ends, which could be related to the nature of the extraction process (Figueroa-Flórez, 2020). Moreover, the particle size of native starch granules varied within an average range of 10-20 μm, which is consistent with the findings reported by Niba *et al*. (2002). Conversely, Anggraini *et al*. (2009) reported an average granule size between 7.3-9.7 μm. This slight difference may be attributed to various factors, such as water stress, environmental conditions, genetics, and the time of crop maturity. Additionally, variations in the processing variables during cassava storage and starch extraction might also contribute to the observed differences.

Non-ultrasonic complexing treatment of starch with lauric acid did not alter the spherical/oval morphology typical of the native structure nor did it produce changes in particle size. However, it caused slight surface lacerations and cavities in some starch granules, such changes could be due to a slight partial gelatinization of the native starches during heating which induced the formation of starch-lauric acid complexes. On the other hand, at higher lauric acid concentrations, some small particles were observed adhering to the granule surface. According to Vasiliadou *et al*. (2015) at heating temperatures below the gelatinization point, amylose leaching in starch granules is reduced. This causes amylose to remain free and attached to the granule surface, which increases its availability to form complexes with lauric acid. Similar results were found for potato starch complexed with fatty acids, finding that the higher the availability of polymeric chains, the higher the formation of lipid films on the granule surface increased (Wang *et al*., 2018).

On the other hand, the ultrasonic treatment reduced the average particle size of the modified starch between 5-15 μm, which is in agreement with the results reported by Falsafi *et al*. (2019). While some dispersed granules retained their smooth surface appearance after the ultrasonic process, others

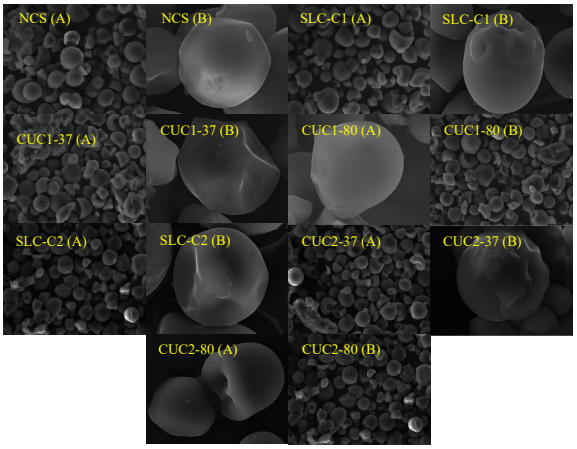

Figure 3. Scanning electron microscopy images of native and modified cassava starch. A: Magnification: 2000X; B: magnification de 15000X. NCS, native cassava starch; SLC-C1, starch-lipid complex with 0.075% lauric acid without ultrasound; SLC-C2, starch-lipid complex with 0.15% lauric acid without ultrasound; CUC1-37, starch-lipid complex with 0.075% lauric acid and ultrasound at 37 kHz; CUC2-37, starch-lipid complex with 0.15% lauric acid and ultrasound at 37 kHz; CUC1-80, starch-lipid complex with 0.075% lauric acid and ultrasound at 80 kHz; CUC2-80, starch-lipid complex with 0.15% lauric acid and ultrasound at 80 kHz.

showed deformed and irregular surfaces or, in certain cases, even suffered total loss of the semi-crystalline structure. Consequently, the presence of minor structural damage served as an indicator of changes in the physicochemical and functional characteristics of the cassava starch samples exposed to ultrasound treatment. Similar characteristics were reported by Jamalabadi *et al*. (2019) for wheat starch after being subjected to ultrasonic treatment. This result may explain why the ultrasonically treated treatments increased the CI of the modified starches and the results in terms of increased relative crystallinity compared to the non-ultrasonically treated complexes.

3.6 Pasting properties

The pasting properties of native cassava starch and starch-lipid complexes are shown in Table 3. Compared to native starch (NCS), modified starches exhibited lower viscosity peaks (PV), suggesting that complex formation may have influenced the molecular interactions between starch chains during swelling (Sun *et al*., 2021). Królikowska *et al*. (2022) also observed a decrease in PV in complexes of cassava and wheat starch with long-chain fatty acids, attributing this trend to the formation of a thin lipid layer that restricts water transfer to the granule, as observed in solubility behavior. Furthermore, it was observed that ultrasonically treated complexes at low frequencies exhibited a decrease in viscosity peaks (PV), while

at higher frequencies, they increased compared to complexes without ultrasonic treatment. This trend has also been reported by other authors, such as Martins *et al*. (2020) on ultrasound-modified starches, indicating that high ultrasonic frequencies can increase the PV of starch. It should be noted that the maximum viscosity is influenced by parameters such as granule size, amylose content, granular swelling capacity, water absorption capacity, semicrystalline order and, the degree of molecular interaction of leached amylose with water molecules.

The breakdown (BD) of lauric acid-treated starch complexes decreased compared to native starch, indicating higher thermal and shear strength stability of modified starch granules after lauric acid treatment with and without an ultrasonic system. It was observed that modified starches with higher lauric acid concentrations and with ultrasonic systems at low frequencies presented higher CI values and in turn showed lower breakdown viscosity. Marinopoulou *et al*. (2016) attributed this effect to the hydrophobicity of the carbon chains present in the complexes, which could hinder the swelling of starch granules during gelatinization. In addition, A. Kaur *et al*. (2007) indicate that higher stability may be related to changes in relative crystallinity and lower swelling of lauric acid-treated starch.

Modification of starch with fatty acids significantly ($p < 0.05$) increased the final viscosity (FV) of starch, possibly due to the solidification of free fatty acids during the cooling step (Wang *et al*., 2016). In addition, the setback (SB) was reduced by up to 23% in the ultrasound-treated starch-lauric acid complexes compared to the native sample, while non-ultrasound treatments only reduced this property by 10.5%. These results indicate that the presence of lipids in starch during the pasting process prevents the reassociation of amylose chains during cooling and storage (Oyeyinka *et al*., 2017). Similar results were found in teff and corn starches complexed with stearic acid by D'Silva *et al*. (2011). The setback and final viscosities are related to the retrogradation and gelling properties of the starch paste, where lower setback viscosity indicates a lower tendency to retrograde and lower gelling ability of the starch paste.

3.7 Thermal properties of starch

Differential Scanning Calorimetry (DSC) analysis corroborates the formation of starch/lipid complexes through the detection of two endothermic peaks: a first peak associated with the dissociation of single amylose helices and disruption of branch points in amylopectin during the gelatinization process; meanwhile, a second endothermic peak appears in modified starches possibly associated with the fusion of the starch/lauric acid complex (Oyeyinka *et al*., 2017). Similar findings have been reported in starches from Vigna subterranean complex with palmitic acid (Oyeyinka *et al*., 2018). The behavior of gelatinization properties in native and lauric acid-modified starches are shown in Table 3. The results evidence that the inclusion of starch/lauric acid complexes significantly increases the gelatinization temperatures (TO, TP, TC) ($p<0.05$). The higher gelatinization temperatures in modified starches can be attributed to the formation of amylose-lipid complexes (SLC-C1, SLC-C2), as evidenced by IC and FTIR-ATR results (Sun *et al*., 2021). On the other hand, the gelatinization enthalpy (ΔH) of the complex was significantly lower concerning native starch ($p < 0.05$), possibly due to an increase in type-I amylose/lipid interactions, coupled with a reduction in the mobility of amylopectin chains precursors of double helix ordering and formation of crystallites of ordered structure (Raza *et al*., 2022).

In addition, the results show an increase in gelatinization temperatures in starches complexed at higher lauric acid concentrations (SLC-C2> SLC-C1). Likewise, they show an increase in TO, TP, and TC in ultrasound-assisted amylose/lipid complexes, being more pronounced at higher ultrasonic frequency intensity (CUC2-80 >CUC2-37; CUC1-80 > CUC1-37).

Table 3. Pasting properties of starch-lauric acid complexes.

CODE	SV	BV	PV	TV	FV	PT
NCS	960.47 ± 5.82^{a}	1777.80 ± 6.30^{a}	2582.33 ± 40.82^{a}	826.53 ± 13.09^{a}	1787.00 ± 7.94^{a}	69.63 ± 0.83^{a}
SLC-C1	791.33 ± 5.13^{b}	748.33 ± 7.64^{b}	2007.67 ± 16.62^{b}	1248.33 ± 7.64^{b}	2039.67 ± 8.74^{b}	90.77 ± 0.95^{b}
CUC1-37	735.33 ± 5.51^{c}	613.33 ± 3.06^{c}	1914.67 ± 5.86^{c}	1301.33 ± 3.51^{cd}	2036.67 ± 4.73^{b}	91.83 ± 0.31^{c}
CUC1-80	787.00 ± 6.08^{bd}	720.00 ± 10.0^{d}	2034.33 ± 14.01^{b}	1314.33 ± 4.04^{df}	2101.33 ± 3.51^{c}	92.50 ± 0.30^{c}
SLC-C2	859.00 ± 4.5^{e}	696.33 ± 4.73^{e}	2033.67 ± 3.21^{b}	1337.33 ± 2.08^{e}	2196.33 ± 5.13^{d}	93.47 ± 0.25^{d}
CUC2-37	777.00 ± 3.61^{d}	656.67 ± 7.64^{f}	1985.67 ± 9.45^{b}	1329.00 ± 4.58^{fe}	2106.00 ± 7.21^{ec}	93.63 ± 0.15^{d}
CUC2-80	828.00 ± 2.00^{f}	825.33 ± 4.51^{g}	2117.33 ± 6.81^{d}	1292.00 ± 2.65^{c}	2120.00 ± 3.00^{e}	93.93 ± 0.15^{d}

SV, setback viscosity; BV, breakdown viscosity; PV, peak viscosity; TV, trough viscosity; FV, final viscosity; PT, pasting temperature. NCS, native cassava starch; SLC-C1, starch-lipid complex with 0.075% lauric acid without ultrasound; SLC-C2, starch-lipid complex with 0.15% lauric acid without ultrasound; CUC1-37, starch-lipid complex with 0.075% lauric acid and ultrasound at 37 kHz; CUC2-37, starch-lipid complex with 0.15% lauric acid and ultrasound at 37 kHz; CUC1-80, starch-lipid complex with 0.075% lauric acid and ultrasound at 80 kHz; CUC2-80, starch-lipid complex with 0.15% lauric acid and ultrasound at 80 kHz.

Table 4. Thermal properties of native and lauric acid-modified starches.

Sample	Peak I				Peak II			
	To	Tp	Tc	ΔH	To	Tp	Tc	ΔH
NCS	64.29±0.06^{a}	68.66±0.12^{a}	86.46±0.08^{a}	19.73±0.14^{a}	ND	ND	ND	ND
SLC-C1	66.12±0,06^{b}	70.91±0.07^{b}	87.77±0.04^{b}	18.45±0.11^{b}	98.23±0.06^{a}	104.30±0.05^{a}	114.85±0.12^{a}	1,59±0.06^{a}
CUC1-37	68.07±0.16^{c}	71.54±0.08^{c}	88.75±0.10^{c}	17.00±0.09^{c}	100.85±0.09^{b}	106.65±0.10^{b}	113.11±0.08^{b}	1.67±0.05^{ab}
CUC1-80	66.79±0.04^{d}	71.30±0.09^{d}	89.15±0.09^{e}	18.12±0.05^{d}	101.24±0.07^{c}	107.12±0.10^{c}	113.91±0.03^{c}	1.81±0.06^{bc}
SLC-C2	66.10±0.13^{b}	71.66±0.06^{c}	88.03±0.11^{f}	17.96±0.14^{d}	99.84±0.11^{d}	107,22±0.04^{c}	114,61±0.05^{a}	1,65±0,06^{a}
CUC2-37	68.44±0.07^{d}	72.23±0.11^{e}	89.30±0.09^{eg}	16.93±0.07^{be}	101.33±0.04^{c}	107.72±0.05^{d}	112.48±0.08^{d}	1.92±0.04^{c}
CUC2-80	68.39±0.05^{d}	72.76±0.06^{f}	89.44±0.09^{g}	16.66±0.14^{e}	102.05±0.06^{e}	108.13±0.04^{e}	113.63±0.53^{bc}	1.87±0.07^{c}

To, onset temperature; Tp, peak temperature Tc, conclusion temperature; ΔH, gelatinization enthalpy. NCS, native cassava starch; SLC-C1, starch-lipid complex with 0.075% lauric acid without ultrasound; SLC-C2, starch-lipid complex with 0.15% lauric acid without ultrasound; CUC1-37, starch-lipid complex with 0.075% lauric acid and ultrasound at 37 kHz; CUC2-37, starch-lipid complex with 0.15% lauric acid and ultrasound at 37 kHz; CUC1-80, starch-lipid complex with 0.075% lauric acid and ultrasound at 80 kHz; CUC2-80, starch-lipid complex with 0.15% lauric acid and ultrasound at 80 kHz.

This variation could be explained by the effect of ultrasonic cavitation on the polymeric chains of the granule, which could cause amylose leaching and a greater interaction between starch and lauric acid, affecting the semicrystalline order and, therefore, the gelatinization properties (Di Marco *et al*., 2023). Similar results have been reported on the formation of starch complexes of lotus root (*Nelumbo nucifera*) induced by ultrasound (Tang *et al*., 2022). However, a significant increase in the melting enthalpy values of the amylose/lipid complex is observed. This result might suggest that the melting enthalpy (ΔH) is the result of the disruption of the individual helices and the crystalline formed by the ordered arrangement of the individual helices with the fatty acid (Wang *et al*., 2020). In this case, the starch/lipid complex must first be broken before the dissociation phenomenon of the arranged helices, therefore, additional energy will be required to break the complexes followed by the thermal degradation action of the amylopectin crystallites. Analogous behavior was reported in waxy rice starches during the formation of amylose/lipid complexes with palmitic acid (Luo *et al*., 2020).

3.8 Solubility in cold water (CWS) and swelling power (SP)

Water solubility (CWS) and swelling power (SP) indicate the extent of interactions between the amorphous and crystalline fractions of starch granules. The results show that the cold-water solubility of modified cassava starches decreased concerning native cassava starches (Table 1). Some authors report that the solubility of native starches is mainly determined by the amylose content because much of it is on the starch surface (Hagenimana & Ding, 2005). Therefore, when native starch forms complexes with a lipophilic molecule it generates a film on the starch surface that is insoluble in water at room temperature, which could explain the decrease in solubility of the complexes for their native counterpart (Faridah *et al*., 2021). The results show that the solubility in cold water decreased when low concentrations of fatty acid were used and when ultrasound treatment was employed. This result may be related to the CI results, which were higher with the use of ultrasound and at lower lauric acid concentrations. Kaur and Singh (2000) indicate that water solubility decreases progressively as the rate of complex formation increases. This statement agrees with the results obtained in the present investigation, where lauric acid-modified starches with higher CI values had lower solubility in cold water. Kaur and Singh (2000) also found a similar trend for complexes formed with cassava starch and oleic acid.

The swelling power of the starch-lipid complexes varied concerning their native counterpart (Table 1). The results showed a decrease in the swelling power of starches after modification by the formation of starch-lipid complexes. This decrease was significant when using ultrasonic treatments and high concentrations of lauric acid during complex formation. Chumsri *et al*. (2022) also found a decrease in the swelling power of rice starches after ultrasound-assisted complex-forming modification. This trend may be because the starch swelling process followed by ultrasonic treatment altered the ordered structure of starch and promoted interactions between amylose-amylose and amylose-amylopectin molecules in starch granules, which could indicate increased water diffusion and low swelling power. Furthermore, this decrease in swelling power at higher lauric acid concentrations was related to CI and peak viscosity of the modified starches. Liu *et al*. (2023) found similar results in the behavior of lauric acid-modified potato, corn, and pea starches.

3.9 In vitro digestibility

The digestibility fractions in native and modified cassava starches obtained by complex formation with lipids are presented in Table 2. The results reveal that NCS samples contain a high fraction of rapidly digested starch (RDS), which is greater than 70%, while the rest of the fractions are divided into slowly digested starch (SDS) and resistant starch (RS) fractions. The results were consistent with reports by K. Liu *et al*., (2018) where the fractions of RDS, SDS, and RS varied in this same proportion. All starch-lauric acid complexes showed decreases in RDS content and exhibited increases in SDS and RS content relative to the native sample, especially complexes

formed at higher lauric acid concentrations, indicating that complexes at higher lipid concentrations might be more resistant to digestion than native starch resulting from partial conversion of RDS to SDS and RS. These results were consistent with those reported previously by Lu *et al*. (2020), Sun *et al*. (2021), and Wu *et al*. (2022), which showed that the degree of digestion of starch-fatty acid complexes was lower than native starch samples. These results may be attributed to the fact that lauric acid, complexed with starch, slows down the action of digestive enzymes and hinders digestion.

As shown in Table 2. compared to the other complexes, starches that were treated with ultrasound exhibited significantly higher RS content, while the untreated ones showed markedly lower RS content. This could be because the ultrasound-treated complexes caused changes in the structural order at both long- and short-range levels than their untreated counterpart. In addition, the ultrasound-assisted starch complexes showed a higher degree of binding to the amylose helical cavity than the untreated ones according to CI and microscopy results. XRD results also showed a well-formed V-type structure, revealing tightly packed individual amylose helices complexed with lauric acid, making them less susceptible to enzymatic attack and slowing down their digestion process. Similar results were reported by Shi *et al*., (2021) who reported that increasing the ultrasonic intensity improved the RS and SDS contents of the wheat starch monoglyceride complex.

On the other hand, starches treated with UT at low frequencies showed results of a greater increase in ADL and AR and a decrease in ADR concerning modified starches at high frequencies, this may be related to more evident structural changes in the starch-lipid complexes formed at frequencies of 37 kHz as shown in the results of IC analysis. Raza *et al*. (2021) indicated that complexes formed with ultrasound at low frequencies caused granular configurations of a more compact starch, exhibiting double helix structures, which caused prevention of the rate of hydrolysis induced by amylolytic enzymes; therefore, subsequently leading to slower hydrolysis of branched chains (amylopectin). Another probable reason could be hydrophobic interactions, which occurred during the formation of the starch-lipid complex, and amylose molecules caused decreasing trends in starch granules' hydration and swelling properties (Shi *et al*., 2021).

Consequently, modifications by starch-lauric acid complex formation resulted in a slowing down of the in vitro digestibility process causing conversions of ADR fractions to ADL and AR. This rate of change was much more severe in starches complexes with higher lauric acid concentrations and treated with ultrasound. This was directly related to the CI, the degree of short-range molecular order, crystallinity, and hydrophobic interactions of the complexes.

Conclusions

Ultrasonic treatment significantly influenced starch modification through complex formation with lauric acid. The best conditions for the formation of starch-lipid complexes with ultrasound were at frequencies of 37 kHz and concentrations of 0.075% lauric acid because these conditions caused alterations in the morphological structure of native starch and led to an improvement in the rate of complex formation between native cassava starch and lauric acid increasing by 22.38%. Furthermore, when ultrasound was applied at low frequency (37 kHz), noticeable changes were observed in the amylose content, crystallinity pattern, and relative crystallinity of native cassava starch. These changes resulted in enhancements in the intrinsic properties of native starch, such as a 27.55% increase in the content of slowly digestible starch (ALD) and an 8.94% increase in resistant starch (AR). Additionally, the starch showed higher stability during heating and a reduced tendency to retrogradation compared to native starch. Based on these results, starch sonication during the formation of starch-lipid complexes played a pivotal role in the modification process, leading to improved CI, pasting, and digestibility properties in native cassava starch. These findings highlight its potential application in the food industry.

Acknowledgment

The authors thank Minciencias (Colombia) for the financial support for this research through the National Fund for Science, Technology, and Innovation of the general royalty's system BPIN (Banco de Programas y Proyectos de Inversión Nacional) 2020000100035

References

Alpizar-Reyes, E., Cruz-Olivares, J., Cortés-Camargo, S., Rodríguez-Huezo, M. E., Macías-Mendoza, J. O., Alvarez-Ramírez, J., & Pérez-Alonso, C. (2022). Structural, physicochemical, and emulsifying properties of pectin obtained by aqueous extraction from red pitaya (*Hylocereus polyrhizus*) peel. *Revista Mexicana de Ingeniería Química 21*(3), 1-22. https://doi.org/10.24275/rmiq/Alim2887

Anggraini, V., Sudarmonowati, E., Hartati, N. S., Suurs, L., & Visser, R. G. F. (2009).

Characterization of cassava starch attributes of different genotypes. *Starch - Stärke 61*(8), 472-481. https://doi.org/10.1002/star.200800121

Arenas, C. and Pedraza, D. (2017). Evaluación del proceso de modificación de almidón de papa mediante acetilación y oxidación, para su aplicación como excipiente en la industria farmacéutica a nivel laboratorio. Tesis de grado en Ingeniería química, Fundación universidad de américa, Colombia

Cao, F., Lu, S., Wang, L., Zheng, M., & Young Quek, S. (2023). Modified porous starch for enhanced properties: Synthesis, characterization and applications. *Food Chemistry 415*, 135765. https://doi.org/10.1016/j.foodchem.2023.135765

Chandak, A., Dhull, S. B., Chawla, P., Fogarasi, M., & Fogarasi, S. (2022). Effect of single and dual modifications on properties of lotus rhizome starch modified by microwave and γ-irradiation: A comparative study. *Foods 11*(19), 2969. https://doi.org/10.3390/foods11192969

Chang, F., He, X., & Huang, Q. (2013). The physicochemical properties of swelled maize starch granules complexed with lauric acid. *Food Hydrocolloids 32*(2), 365-372. https://doi.org/10.1016/j.foodhyd.2013.01.021

Chumsri, P., Panpipat, W., Cheong, L.-Z., & Chaijan, M. (2022). Formation of intermediate amylose rice starch-lipid complex assisted by ultrasonication. *Foods 11*(16), 2430. https://doi.org/10.3390/foods11162430

D'Silva, T. V., Taylor, J. R. N., & Emmambux, M. N. (2011). Enhancement of the pasting properties of teff and maize starches through wet-heat processing with added stearic acid. *Journal of Cereal Science 53*(2), 192-197. https://doi.org/10.1016/j.jcs.2010.12.002

Dewi, A. M. P., Santoso, U., Pranoto, Y., & Marseno, D. W. (2022). Dual modification of sago starch via heat moisture treatment and octenyl succinylation to improve starch hydrophobicity. *Polymers 14*(6), 1086. https://doi.org/10.3390/polym14061086

Di Marco, A. E., Ixtaina, V. Y., & Tomás, M. C. (2023). Effect of ligand concentration and ultrasonic treatment on inclusion complexes of high amylose corn starch with chia seed oil fatty acids. *Food Hydrocolloids 136*, 108222. https://doi.org/10.1016/j.foodhyd.2022.108222

Falsafi, S. R., Maghsoudlou, Y., Aalami, M., Jafari, S. M., & Raeisi, M. (2019). Physicochemical and morphological properties of resistant starch type 4 prepared under ultrasound and conventional conditions and their *in vitro* and *in vivo* digestibilities. *Ultrasonics Sonochemistry 53*, 110-119. https://doi.org/10.1016/j.ultsonch.2018.12.039

Faridah, D. N., Andriani, I., Talitha, Z. A., & Budi, F. S. (2021). Physicochemical characterization of resistant starch type V (RS5) from manggu cassava starch (*Manihot esculenta*). *Food Research 5*(2), 228-234. https://doi.org/10.26656/fr.2017.5(2).496

Figueroa-Flórez, J. (2020). Procesos de biocátalisis enzimática en almidones nativos y pre-gelatinizados de yuca: Efectos a nivel morfológico, molecular y de digestibilidad in vitro. Tesis de doctorado en Biotecnología, Universidad Nacional de Colombia, Colombia

Ge, X., Shen, H., Sun, X., Liang, W., Zhang, X., Sun, Z., Lu, Y., & Li, W. (2022). Insight into the improving effect on multi-scale structure, physicochemical and rheology properties of granular cold water soluble rice starch by dielectric barrier discharge cold plasma processing. *Food Hydrocolloids 130*, 107732. https://doi.org/10.1016/j.foodhyd.2022.107732

Golkar, A., Milani, J. M., Motamedzadeghan, A., & Kenari, R. E. (2023). Physicochemical, structural, and rheological characteristics of corn starch after thermal-ultrasound processing. *Food Science and Technology International 29*(2), 168-180. https://doi.org/10.1177/10820132211069242

Hagenimana, A., & Ding, X. (2005). A comparative study on pasting and hydration properties of native rice starches and their mixtures. *Cereal Chemistry Journal 82*(1), 70-76. https://doi.org/10.1094/CC-82-0070

Jamalabadi, M., Saremnezhad, S., Bahrami, A., & Jafari, S. M. (2019). The influence of bath and probe sonication on the physicochemical and microstructural properties of wheat starch. *Food Science & Nutrition 7*(7), 2427-2435. https://doi.org/10.1002/fsn3.1111

Jin, Z. (Ed.). (2018). *Functional Starch and Applications in Food*. Springer Singapore. https://doi.org/10.1007/978-981-13-1077-5

Kang, X., Liu, P., Gao, W., Wu, Z., Yu, B., Wang, R., Cui, B., Qiu, L., & Sun, C. (2020). Preparation of starch-lipid complex by ultrasonication and its film forming capacity. *Food Hydrocolloids 99*, 105340. https://doi.org/10.1016/j.foodhyd.2019.105340

Kaur, A., Singh, N., Ezekiel, R., & Guraya, H. S. (2007). Physicochemical, thermal and pasting properties of starches separated from different potato cultivars grown at different locations. *Food Chemistry 101*(2), 643-651. https://doi.org/10.1016/j.foodchem.2006.01.054

Kaur, K., & Singh, N. (2000). Amylose-lipid complex formation during cooking of rice flour. *Food Chemistry 71*(4), 511-517. https://doi.org/10.1016/S0308-8146(00)00202-8

Królikowska, K., Pietrzyk, S., Pustkowiak, H., & Wolak, K. (2022). The effect of cassava and wheat starches complexation with selected fatty acids on their functional properties. *Journal of Food Science and Technology 59*(4), 1440-1449. https://doi.org/10.1007/s13197-021-05153-x

Li, Q., Dong, Y., Gao, Y., Du, S., Li, W., & Yu, X. (2021). Functional properties and structural characteristics of starch-fatty acid complexes prepared at high temperature. *Journal of Agricultural and Food Chemistry 69*(32), 9076-9085. https://doi.org/10.1021/acs.jafc.1c00110

Li, X., Gao, X., Lu, J., Mao, X., Wang, Y., Feng, D., Cao, J., Huang, L., & Gao, W. (2019). Complex formation, physicochemical properties of different concentration of palmitic acid yam (*Dioscorea pposita* Thunb.) starch preparation mixtures. *LWT 101*(November 2018), 130-137. https://doi.org/10.1016/j.lwt.2018.11.032

Liu, K., Zu, Y., Chi, C., Gu, B., Chen, L., & Li, X. (2018). Modulation of the digestibility and multi-scale structure of cassava starch by controlling the cassava growth period. *International Journal of Biological Macromolecules 120*, 346-353. https://doi.org/10.1016/j.ijbiomac.2018.07.184

Liu, Q., Wang, Y., Yang, Y., Yu, X., Xu, L., Jiao, A., & Jin, Z. (2023). Structure, physicochemical properties and in vitro digestibility of extruded starch-lauric acid complexes with different amylose contents. *Food Hydrocolloids 136*(March 2022), 108239. https://doi.org/10.1016/j.foodhyd.2022.108239

Lu, X., Liu, H., & Huang, Q. (2020). Fabrication and characterization of resistant starch stabilized Pickering emulsions. *Food Hydrocolloids 103*, 105703. https://doi.org/10.1016/j.foodhyd.2020.105703

Luo, S., Zeng, Z., Mei, Y., Huang, K., Wu, J., Liu, C., & Hu, X. (2020). Improving ordered arrangement of the short-chain amylose-lipid complex by narrowing molecular weight distribution of short-chain amylose. *Carbohydrate Polymers 240*, 116359. https://doi.org/10.1016/j.carbpol.2020.116359

Marinopoulou, A., Papastergiadis, E., & Raphaelides, S. N. (2016). An investigation into the structure, morphology and thermal properties of amylomaize starch-fatty acid complexes prepared at different temperatures. *Food Research International 90*, 111-120. https://doi.org/10.1016/j.foodres.2016.10.035

Martins, A., Beninca, C., Bet, C. D., Bisinella, R. Z. B., de Oliveira, C. S., Hornung, P. S., & Schnitzler, E. (2020). Ultrasonic modification of purple taro starch (*Colocasia esculenta* B. Tini): structural, psychochemical and thermal properties. *Journal of Thermal Analysis and Calorimetry 142*(2), 819-828. https://doi.org/10.1007/s10973-020-09298-3

Méndez, P. A., Méndez, Á. M., Martínez, L. N., Vargas, B., & López, B. L. (2022). Cassava and banana starch modified with maleic anhydride-poly (ethylene glycol) methyl ether (Ma-mPEG): A comparative study of their physicochemical properties as coatings. *International Journal of Biological Macromolecules 205*(January), 1-14. https://doi.org/10.1016/j.ijbiomac.2022.02.053

Niba, L. L., Bokanga, M. M., Jackson, F. L., Schlimme, D. S., & Li, B. W. (2002). Physicochemical properties and starch granular characteristics of flour from various *Manihot esculenta* (Cassava) Genotypes. *Journal of Food Science 67*(5), 1701-1705. https://doi.org/10.1111/j.1365-2621.2002.tb08709.x

Oyeyinka, S. A., Adegoke, R., Oyeyinka, A. T., Salami, K. O., Olagunju, O. F., Kolawole, F. L., Joseph, J. K., & Bolarinwa, I. F. (2018). Effect of annealing on the functionality of Bambara groundnut (*Vigna subterranea*) starch-palmitic acid complex. *International Journal of Food Science & Technology 53*(2), 549-555. https://doi.org/10.1111/ijfs.13635

Oyeyinka, S. A., Kayitesi, E., Diarra, S. S., Adedeji, A. A., Amonsou, E. O., & Singh, S. (2021). Bambara Groundnut Starch. In *Food and Potential Industrial Applications of Bambara Groundnut* (pp. 85-118). Springer International Publishing. https://doi.org/10.1007/978-3-030-73920-1_6

Oyeyinka, S. A., Singh, S., Venter, S. L., & Amonsou, E. O. (2017). Effect of lipid types on complexation and some physicochemical properties of bambara groundnut starch. *Starch/Staerke 69*(3-4), 1-10. https://doi.org/10.1002/star.201600158

Raza, H., Ameer, K., Ren, X., Liang, Q., Chen, X., Chen, H., & Ma, H. (2021). Physicochemical properties and digestion mechanism of starch-linoleic acid complex induced by multi-frequency power ultrasound. *Food Chemistry 364*(February), 130392. https://doi.org/10.1016/j.foodchem.2021.130392

Raza, H., Liang, Q., Ameer, K., Ma, H., & Ren, X. (2022). Dual-frequency power ultrasound effects on the complexing index, physicochemical properties, and digestion mechanism of arrowhead starch-lipid complexes. *Ultrasonics Sonochemistry 84*, 105978. https://doi.org/10.1016/j.ultsonch.2022.105978

Reyes, I., Rodríguez-Huezo, M. E., & Garcia-Diaz, S. (2023). Opuntia ficus-indica mucilage reduces wheat starch in vitro digestibility. *Revista Mexicana de Ingeniería Química 22*(2), 1-10. https://doi.org/10.24275/rmiq/Alim2316

Rolland-Sabaté, A., Sánchez, T., Buléon, A., Colonna, P., Jaillais, B., Ceballos, H., & Dufour, D. (2012). Structural characterization of novel cassava starches with low and high-amylose contents in comparison with other commercial sources. *Food Hydrocolloids 27*(1), 161-174. https://doi.org/10.1016/j.foodhyd.2011.07.008

Salgado-Delgado, A. M., Lozano-Pineda, E., Salgado-Delgado, R., Hernández-Uribe, J. P., Olarte-Paredes, A., & Granados-Baeza, M. J. (2022). Chemical modification of rice (*Oryza sativa*) and potato (*Solanum tuberosum*) starches by silanization with trimethoxy(methyl)silane. *Revista Mexicana de Ingeniería Química 21*(3), 1-16. https://doi.org/10.24275/rmiq/Alim2802

Serna-Fadul, T. (2022). Desarrollo de una premezcla en polvo para pandebono con incorporación de harina modificada de yuca (*Manihot esculenta*) y componentes bioactivos de harina nativa de ahuyama (*Cucurbita* spp.). Tesis de maestría en Ingeniería Agroindustrial, Universidad Nacional de Colombia, Colombia.

Shi, M., Wang, F., Lan, P., Zhang, Y., Zhang, M., Yan, Y., & Liu, Y. (2021). Effect of ultrasonic intensity on structure and properties of wheat starch-monoglyceride complex and its influence on quality of norther-style Chinese steamed bread. *LWT 138*, 110677. https://doi.org/10.1016/j.lwt.2020.110677

Sun, S., Jin, Y., Hong, Y., Gu, Z., Cheng, L., Li, Z., & Li, C. (2021). Effects of fatty acids with various chain lengths and degrees of unsaturation on the structure, physicochemical properties and digestibility of maize starch-fatty acid complexes. *Food Hydrocolloids 110*, 106224. https://doi.org/10.1016/j.foodhyd.2020.106224

Tang, J., Liang, Q., Ren, X., Raza, H., & Ma, H. (2022). Insights into ultrasound-induced starch-lipid complexes to understand physicochemical and nutritional interventions. *International Journal of Biological Macromolecules 222*(PA), 950-960. https://doi.org/10.1016/j.ijbiomac.2022.09.242

Tufvesson, F., Wahlgren, M., & Eliasson, A.-C. (2003). Formation of amylose-lipid complexes and effects of temperature treatment. Part 2. Fatty acids. *Starch - Stärke 55*(34), 138-149. https://doi.org/10.1002/star.200390028

Vasiliadou, E., Raphaelides, S. N., & Papastergiadis, E. (2015). Effect of heating time and temperature on partially gelatinized starch-fatty acid interactions. *LWT - Food Science and Technology 60*(2), 698-707. https://doi.org/10.1016/j.lwt.2014.10.026

Wang, H., Xu, K., Ma, Y., Liang, Y., Zhang, H., & Chen, L. (2020). Impact of ultrasonication on the aggregation structure and physicochemical characteristics of sweet potato starch. *Ultrasonics Sonochemistry 63*, 104868. https://doi.org/10.1016/j.ultsonch.2019.104868

Wang, L., Wang, W., Wang, Y., Xiong, G., Mei, X., Wu, W., Ding, A., Li, X., Qiao, Y., & Liao, L. (2018). Effects of fatty acid chain length on properties of potato starch-fatty acid complexes under partially gelatinization. *International Journal of Food Properties 21*(1), 2121-2134. https://doi.org/10.1080/10942912.2018.1489842

Wang, S., Chao, C., Cai, J., Niu, B., Copeland, L., & Wang, S. (2020). Starch-lipid and starch-lipid-protein complexes: A comprehensive review. *Comprehensive Reviews in Food Science and Food Safety 19*(3), 1056-1079. https://doi.org/10.1111/1541-4337.12550

Wang, S., Wang, J., Yu, J., & Wang, S. (2016). Effect of fatty acids on functional properties of normal wheat and waxy wheat starches: A structural basis. *Food Chemistry 190*, 285-292. https://doi.org/10.1016/j.foodchem.2015.05.086

Wu, X., Jiang, Y., Wang, X., Fang, Y., Lin, Q., & Ding, Y. (2022). Structural and *in vitro* starch digestion properties of starch-fatty acid nanocomplexes: effect of chain lengths and degree of unsaturation of fatty acids. *Journal of the Science of Food and Agriculture 102*(15), 7239-7248. https://doi.org/10.1002/jsfa.12089

Xiao, Y., Wu, X., Zhang, B., Luo, F., Lin, Q., & Ding, Y. (2021). Understanding the aggregation structure, digestive and rheological properties of corn, potato, and pea starches modified by ultrasonic frequency. *International Journal of Biological Macromolecules 189*, 1008-1019. https://doi.org/10.1016/j.ijbiomac.2021.08.163

Zabar, S., Lesmes, U., Katz, I., Shimoni, E., & Bianco-Peled, H. (2010). Structural characterization of amylose-long chain fatty acid complexes produced via the acidification method. *Food Hydrocolloids 24*(4), 347-357. https://doi.org/10.1016/j.foodhyd.2009.10.015

Zhang, J., Ran, C., Jiang, X., & Dou, J. (2021). Impact of octenyl succinic anhydride (OSA) esterification on microstructure and physicochemical properties of sorghum starch. *Lwt 152*(June), 112320. https://doi.org/10.1016/j.lwt.2021.112320

Zhong, Y., Bertoft, E., Li, Z., Blennow, A., & Liu, X. (2020). Amylopectin starch granule lamellar structure as deduced from unit chain length data. *Food Hydrocolloids 108*, 106053. https://doi.org/10.1016/j.foodhyd.2020.106053

Zhou, Z., Liang, Z., Zhang, Y., Hu, H., Gan, T., & Huang, Z. (2023). Facile solid-phase synthesis of starch-fatty acid complexes via mechanical activation for stabilizing curcumin-loaded Pickering emulsions. *Food Research International 166*, 112625. https://doi.org/10.1016/j.foodres.2023.112625TT